

Photocatalytic decolorization of Methylene Blue by using solid-state zinc exchanged clinoptilolite

Faezeh Jafarpisheh^a, Mohammad Ghorbanpour^{b,*}

^aTechnical and Engineering Faculty, University of Mohaghegh Ardabili, Ardabil, Iran, email: micromahkameh@gmail.com

^bFaculty of Chemical and Petroleum Engineering, University of Tabriz, Tabriz, Iran, email: Ghorbanpour@tabrizu.ac.ir

Received 10 August 2022; Accepted 6 February 2023

ABSTRACT

Zinc ion-exchanged clinoptilolite samples were prepared by reaction of different concentrations of clinoptilolite and zinc chloride (10%–40%) using solid phase ion-exchange method. The samples were characterized by X-ray diffraction spectroscopy, Fourier-transform infrared spectroscopy (FTIR), Brunauer–Emmett–Teller, energy-dispersive X-ray spectroscopy and scanning electron microscopy spectroscopy. A UVA lamp was then employed to irradiate UV light on the solution of Methylene Blue (MB) and photocatalyst at room temperature. The degradation percentage was calculated by assessing its absorbance using an ultraviolet-visible spectrophotometer. Regarding 30% and 40% samples, the amount of transferred zinc almost remained steady. Specific areas of the sample surface have been modified by a similar method. After ion-exchange occurred, photocatalytic activity of clinoptilolite changed slightly. These changes were regarding the shape, crystalline phase and FTIR spectra of samples. When pH = 3 and 10 g/L modified zeolite was used as catalyst, the photocatalytic decolorization rate of MB dye was observed the highest, which was 95.4%. The results show that the reuse of photocatalyst is possible. The outcomes demonstrate that it is possible to reuse the photocatalyst, which is significant for real-world applications.

Keywords: Photocatalytic decolorization; Solid-state ion-exchange; Zinc; Clinoptilolite

1. Introduction

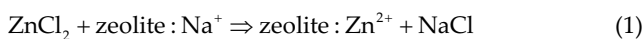
When dyes are present in wastewater effluents, they can cause chemical reactions, oxidation, and hydrolysis which will consequently result in highly toxic compounds. These compounds can directly or indirectly harm human beings by causing allergies, tumors, and also cancer [1]. Dyes block light from entering the water, which affects the photosynthetic activity. Methylene Blue dye which is often used in industries that are involved with materials such as wood, plastics and silk. However, it is a cationic dye with a complicated structure, low decomposition rate and intense resistant to heat and light which endangers animals and also human beings health [2,3]. As a result, numerous studies have been done regarding decontamination of this dye from

industrial effluent using a variety of methods, for example, membrane separation, coagulation, adsorption and aerobic or anaerobic treatments [4]. Since organic compounds have efficiently broken into smaller compounds such as CO₂, H₂O, and small molecules, heterogeneous photocatalytic oxidation has attracted great attention for the destructive of dyes and textile effluents [5]. ZnO nanoparticles are one of the most favorable materials amongst photocatalysts for it is non-toxic, insoluble, stable, highly photo-active, and is also economic [6]. The ZnO nanoparticles, however, often have small particle sizes, making them hard to be collected from suspensions using practical methods such as filtration. For overcoming such obstacles, ZnO-support composites could be used on different substrates such as activated carbon [7,8], zeolites [2,9], clays [10,11] and silica [12,13] are used.

* Corresponding author.

Among them, natural zeolites are known to be a preferable choice for controlling pollution due to their ion-exchange capability, cost-effectiveness and being available globally [2]. These features make zeolites particularly beneficial for being used in reactions leading to ion-exchange, adsorption, or molecular sieves to remove a variety of harmful compounds including heavy metals or hydrocarbons from wastewaters [14]. Clinoptilolite, a type of natural zeolite that belongs to the heulandite group, is one of the most common and widely utilized zeolite minerals. Two-dimensional channels in their three-dimensional crystal structure hold several ion-exchangeable cations such as Na^+ , K^+ , Ca^{2+} , and Mg^{2+} [15,16]. These cations could either exchanged with organic or inorganic ions.

Natural zeolites need modifications regarding their composition, structural and crystal size and shape in order to be used as catalysts. The required qualifications are achieved using methods such as ion-exchange and de-alumination. The $\text{SiO}_2/\text{Al}_2\text{O}_3$ ratio of zeolites is raised through de-alumination. Even in cases where the material's overall composition hasn't changed or has just slightly changed, this phrase is typically understood to refer to the displacement of aluminum from the zeolite structure [17]. Being compared with de-alumination, due to the enormous amounts of the material that are accessible and its low price, ion-exchange on natural zeolites appears to be a more appealing option [2]. Conventional ion-exchange techniques used for clays mostly occur in liquid-state reactions. Such techniques usually require unfavorable conditions for instance high reaction temperatures and renewal of solutions in which metals are exchanged [18]. Overcoming such challenges, some researchers used solid-state processes instead [18–20]. A solid-state process is done by mixing and then heating zeolite with a suitable salt such as ZnCl_2 in a furnace up to its melting point. Ion-exchange happens by molten salt medium penetrating pores of zeolite and the reaction is as represented:



This approach is simple and fast, compared to liquid-state methods and is used for synthesis of photocatalyst, adsorbent, and antibacterial, metal/clay composites [21,22].

Hajipour et al. [23] synthesized bentonite/copper catalysts using solid-phase ion-exchange at different temperatures (200°C and 300°C) and different time periods (2 and 10 min). These catalysts were used as heterogeneous catalysts for photo Fenton treatment of methyl orange under UV irradiation. The sample which was prepared at 200°C for 10 min was selected as the optimum sample. Shayegh and Ghorbanpour [24] used the same method to assess the bentonite/Fe dye adsorption. Hakimi et al. [11] investigated the photocatalytic behavior of bentonite/zinc particles. The particles were obtained by ion-exchange process in both solid-state and liquid-state. They reported that solid-state ion-exchange had the higher decolorization efficiency.

Thus far, no study appears to be published aiming photocatalytic-activity of zinc modified zeolites using this method. Since clinoptilolite is abundant and inexpensive, the current study was to modify it using solid state

ion-exchange techniques and to investigate decolorization characteristics of the dye. The modified zeolite catalyst is then characterized.

2. Experimental

Methylene Blue (MB), HCl, NaOH and ZnCl_2 were purchased from Merck Co.

2.1. Synthesis of zinc exchanged clinoptilolite

Clinoptilolite and the appropriate concentrations of ZnCl_2 (10, 20, 30, and 40% w/w) were thoroughly mixed. Samples were labeled as 10, 20, 30, and 40, respectively. Then the resulting mixture is heated for 60 min at 300°C in a furnace. The resulting samples were thoroughly cleaned with distilled water, after and were dried in an oven at 25°C after being dissolved.

2.2. Photocatalytic decolorization efficiency

Photo-activity of samples was indicated by Methylene Blue with an initial concentration 300 ppm and volume of and 50 mL. A UVA lamp (5 W, Philips, Netherlands) was employed to irradiate a solution of MB and photocatalyst (10 g/L) at room temperature. The solution was then immediately centrifuged following the reaction. Its absorbance was calculated using a UV-visible spectrophotometer for determining the percentage of degradation. Eq. (2) is used to compute the efficiency of photocatalytic degradation:

Photocatalytic decolorization

$$\text{efficiency}(\%) = \left(\frac{A_0 - A}{A_0} \right) \times 100 \quad (2)$$

where A_0 is the initial dye solution absorption and A is the initial absorption following irradiation.

2.3. Characterization

A LEO 1430VP instrument was used to conduct scanning electron microscopy (SEM) and energy-dispersive X-ray spectroscopy (EDX) (LEO 1430VP, Germany). A PW 1050 X-ray diffractometer (Philips, The Netherlands) was used to conduct the powder X-ray diffraction investigation. Materials with N_2 adsorption/desorption were assessed using a Micromeritics Brunauer–Emmett–Teller (BET) surface area and porosity analyzer (Gemini 2375, Germany) in the relative pressure range of 0.05–1.00 at a constant temperature of 77 K. Fourier-transform infrared spectroscopy (FTIR) assessed the functional groups influencing the adsorption process in the frequency range of 400–4,000 cm^{-1} , using a PerkinElmer spectrophotometer.

3. Results and discussion

3.1. Photocatalytic decolorization efficiency

The results illustrated that prepared ion-exchanged samples have diverse photocatalytic decolorization efficiencies

(Fig. 1). The photocatalytic decolorization efficiency of samples 10, 20, 30, and 40, in comparison with, were 73.4%, 86.9%, 95.4% and 96.0%, respectively. Thus, it was discovered that addition of more amount of salt to the initial mixture leads to greater photocatalytic values. Hence, it was observed that samples 30 and 40 had the same photocatalytic decolorization efficiency. The optimized sample was considered to be sample 30. By considering the amount of dye concentration in aqueous solution (300 mg/L), it can be said that the performance of the synthesized photocatalyst is comparable with the best results reported in literature, while the production method was low-cost, fast and relatively simple to perform [7,10,13].

3.2. Characterization

Fig. 2 shows the SEM images of the parent clinoptilolite and sample 30. As demonstrated, clinoptilolite is consisted of fine-graining particles with uneven surfaces that have a lamellar texture. On the other hand, these particles are

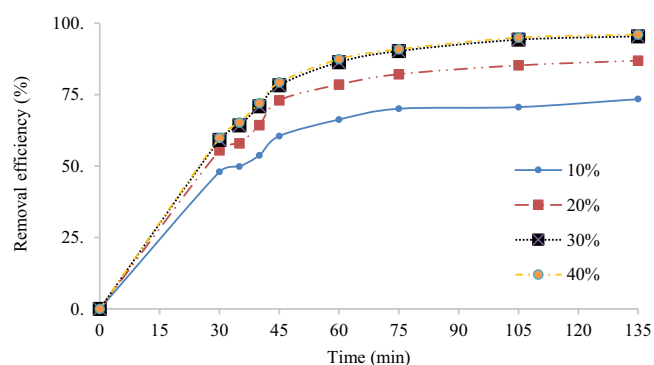


Fig. 1. Photocatalytic degradation efficiency of parent clinoptilolite and prepared ion-exchanged samples.

adhered and have created agglomerated forms. The clinoptilolite particles lacked any uniform shape. Minute changes to the original clinoptilolite's appearance were observed after the ion-exchange procedure.

Table 1 represents the results of EDX analysis on parent clinoptilolite and ion-exchanged samples. Sodium, magnesium, potassium, calcium, and iron were the dominant cations in samples. Meanwhile ion-exchange process occurred; clinoptilolite's Zn^{2+} ions replaced exchangeable cations, resulting in an improved zeolite with higher zinc amount and lower Na, K, Ca, and Mg amount than the parent clinoptilolite. There was no zinc content observed in the parent clinoptilolite whereas it was reported 2.83% in sample 10 and 4.06% in sample 20. This percentage rose to 5.38% in sample 30. As the salt amount in the initial mixture increased, to 40%, the zinc amount rises to 5.69%, as well. This is almost equivalent amount reported for sample 30. In other words, it can be mentioned that addition of 30% zinc chloride salt to the initial mixture results in an

Table 1
Energy-dispersive X-ray spectroscopy analysis of parent clinoptilolite and ion-exchanged samples

Sample	0	10	20	30	40
Oxygen	52.76	54.21	55.8	55.34	54.69
Sodium	2.12	0	0	0	0
Magnesium	0.43	0.34	0.22	0.28	0.22
Aluminum	6.36	6.3	5.9	5.78	5.86
Silicon	35.6	33.55	31.25	30.87	31.49
Potassium	1.02	1.13	1.19	0.87	0.84
Calcium	0.90	0.81	0.89	0.76	0.76
Iron	0.81	0.83	0.69	0.72	0.45
Zinc	0	2.83	4.06	5.38	5.69

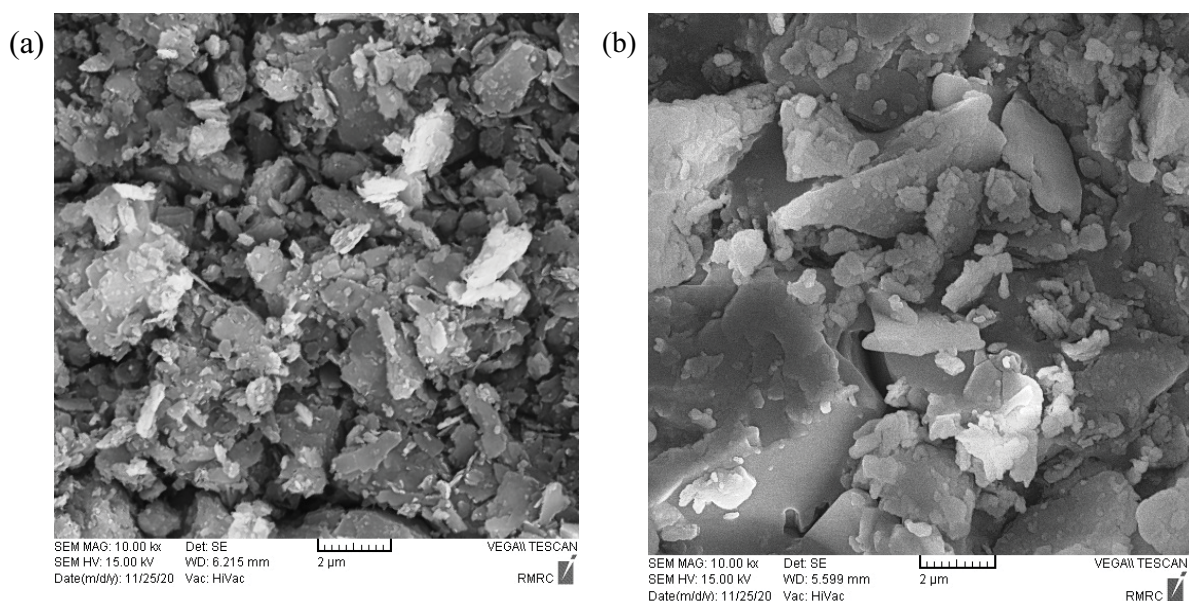


Fig. 2. Scanning electron microscopy images of parent clinoptilolite (a) and sample 30 (b).

approximate saturation of zeolite. Further addition has no impact on ion-exchange.

Fig. 3 shows the X-ray diffraction (XRD) patterns of parent clinoptilolite and the ion-exchanged samples. The XRD analysis shows three peaks which indicate clinoptilolite features ($2\theta = 10.06^\circ$, 22.66° , and 30.38°) [16]. Furthermore, it shows the existence of additional phases which are considered as impurities, for instance mordenite and quartz. The patterns related to the ion-exchanged samples also indicated similar diffraction peaks. In other words, quartz phase, which shouldn't be impacted by ion-exchange process, was observed. The spectra illustrates that ion-exchange had no noticeable impact on the parent clinoptilolite's structure. Peak positions and intensities were slightly decreased as a result of the collapse of porous structure. This collapse happens during the ion-exchange process and mesoporous channels are distorted.

Fig. 4 depicts the FTIR spectra of the parent clinoptilolite and sample 30. Discrete water absorption bands demonstrated in the FTIR measurements show how extensively the parent clinoptilolite is hydrated. These common bands involve the vibration of the OH–O bonds at $3,450\text{ cm}^{-1}$, the bridging OH groups in Al–OH–Si groups at $3,615$ and $1,660\text{ cm}^{-1}$. The mentioned bands are in reference to the water molecules connected to the cations that are already in the structure of zeolite channels [15]. Both the original clinoptilolite and the ion-exchanged sample demonstrate the infrared signals for Si–O–Al asymmetrical stretching ($1,034\text{ cm}^{-1}$), Si–O bending (469 cm^{-1}), O–Si–O bending (606 cm^{-1}), Si–O

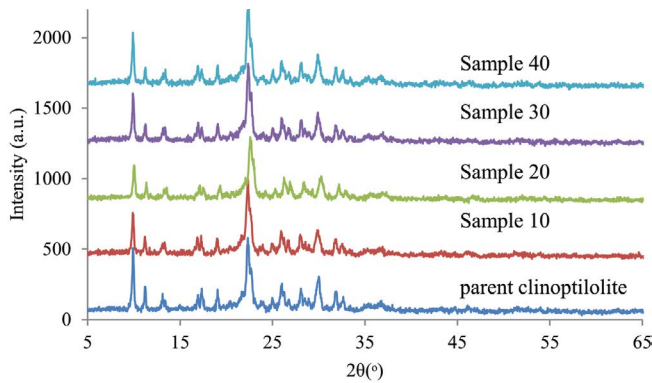


Fig. 3. X-ray diffraction pattern of parent clinoptilolite and ion-exchanged samples.

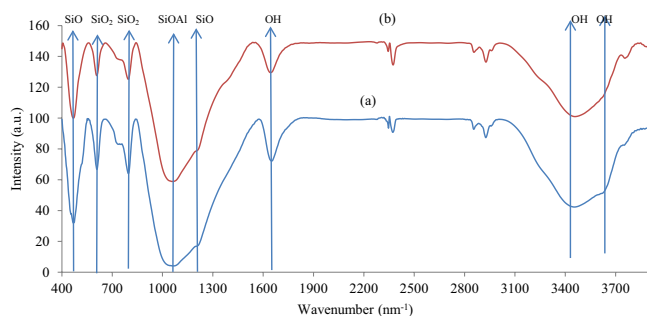


Fig. 4. Fourier-transform infrared spectra of parent clinoptilolite (a) and sample 30 (b).

asymmetric stretching ($1,217\text{ cm}^{-1}$), and O–Si–O symmetric stretching (796 cm^{-1}) [16]. It is noteworthy to mention that the Si–O and O–Al bond intensities, which are typical of tectosilicates, are high, illustrating that the zeolite has an enormous surface area [9]. Additionally, the peaks at 524 and 746 cm^{-1} were also observed. This corresponds to the “pore opening” vibration and the symmetric stretching of free SiO_4 , respectively. These findings agree with those of other researchers [15]. Regarding the intensities and wave numbers given in FTIR spectra of both parent clinoptilolite and ion-exchanged samples, following ion-exchange has no effect on them (the spectrum of other samples was also similar to the sample 30 and is not given). The values of the peaks between $3,615$ and $1,660\text{ cm}^{-1}$ in the Zn exchanged sample underwent a fall. This may be as a result of heating the mixture during the process [16].

Table 2 shows BET analysis of parent and ion-exchanged clinoptilolite. Along the ion-exchange procedure, the BET surface area rose from 12.40 to $15.52\text{ m}^2/\text{g}$. As surface fractures are formed, the pore structure collapsing during this process. Pure clinoptilolite pores are 12.2 \AA regarding their size. They are arranged in regular arrays and are of the same size. On the other hand, as the Zn^{2+} exchange mechanism occurs, displacement of two Na^+ cations by one Zn^{2+} cation is expected leading to increased pore size and surface area.

As reported, the efficiency of the photocatalytic processes depends on the amount of semiconductor supported on zeolite [11]. The EDX results revealed that by increasing zinc chloride amount in the initial ion-exchange mixture, the amount of exchanged zinc in clinoptilolite increases as well. In other hand, after ion-exchange, the parent clinoptilolite's shape, crystalline phase, and FTIR spectra were remarked with minor changes. Incrementation of the photocatalytic efficiency by addition of higher amount of zinc can be explained by the optical properties of the photocatalyst. Indeed, the total active surface area was increased by up going of catalyst dosage. In this case more photons can be absorbed by the present catalyst particles. This rises the quantity of hydroxyl and superoxide radicals. However, the amount of zinc that was exchanged was nearly the same as samples 30 and 40 (Table 1). Hence, samples 30 and 40 had the same photocatalytic decolorization efficiency. A similar process has been done on the specific area of the sample's surface (Table 2). In conclusion and due to the mentioned findings, sample 30 has the highest photocatalytic decolorization efficiency possible.

3.3. Optimization the photocatalytic decolorization efficiency

Fig. 5 shows impacts of the initial pH on the photo-degradation efficiency considering sample 30 as the optimum

Table 2
Brunauer–Emmett–Teller analysis of parent clinoptilolite and ion-exchanged samples

Sample	0	10	20	30	40
V_p ($\text{cm}^3\cdot\text{g}^{-1}$)	0.015564	0.031897	0.030825	0.027684	0.030741
$r_{p,\text{peak}}$ (nm)	1.22	1.66	1.88	1.66	1.7975
a_p ($\text{m}^2\cdot\text{g}^{-1}$)	12.402	15.278	14.685	14.765	15.52175

sample. As a result, pH = 3 had the highest dye photocatalytic degradation effectiveness which ranged from 93.1% at pH = 3 to 80.5% at pH = 5.

Finding the ideal catalyst dosage is one of the key variables in photocatalytic experiments. According to the findings given in Fig. 6, increasing the catalyst dose from 5 to 10 g/L results in a rise in the photocatalytic degradation of the dye from 85.4 to 96.6% and then it stays steady. Addition of more photocatalyst material increases the quantity of available catalyst sites which brings more dye molecules near hydroxyl radicals on surface of the catalyst [25,26]. In this case, faster reaction of hydroxyl radicals with pollutants molecules takes place due to low life time of hydroxyl radicals. By increasing in the catalyst dosage, the available active sites can also increase, hence more hydroxyl radicals will produce. Further increase in the weight of the catalyst showed a negative effect. On the other hand, at higher doses, beyond the optimum value, some parts of the catalyst are in the dark causing a decrease in the light penetration. Light scattering is another reason for decreasing in the catalyst efficiency at higher catalyst dosage. Therefore, at 10 g/L of the modified zeolite, the photocatalytic degradation of Methylene Blue dye achieved the maximum rate of efficiency.

Fig. 7 investigates the photocatalytic degradation effectiveness of the optimized sample with dye concentrations of 300–600 mg/L at pH = 3 and an adsorbent dose of 10 g/L. According to this, raising concentration of dye leads to a drop in the dye's photocatalytic degradation efficiency. On

top of the results, the efficiency of dye removal is reduced from 95.4% to 79.3% when the dye concentration increased from 300 to 600 ppm. If the dye concentration is high, it can reduce transparency of the solution and act as a filter that barrier light reaching the photocatalyst. Therefore, the desired light intensity will not be able to reach the catalyst surface in a specific time period; Thus, photocatalytic degradation decreases. In these conditions, more dye molecules will be adsorbed on the surface of the photocatalyst therefore the active sites of the catalyst will be reduced. In other words, the aforementioned increase the number of substrate ions accommodating in inter layer spacing and inhibit the action of catalyst which thereby decreases the reactive free radicals attacking the dye molecules and photocatalytic degradation efficiency [11].

In a recent research, Costa-Marrero et al. [2] have added Zn²⁺ exchanged natural clinoptilolite in a 80 mL and 2 ppm MB solution to assess its adsorption and revealed a 90% range of adsorption. Although the present study assessed the photocatalytic degradation procedure, a higher decomposition efficient was resulted which is significant in comparison with the aforementioned study. Hakimi et al. [11] have reported a 87% decomposition rate for methyl orange solution using ZnO/bentonite (1 g/L). The present study has revealed that presence of 10 g/L catalyst can degrade about 80% of 600 mg/L dye solution. It can be said that the performance of the synthesized solid-state zinc exchanged clinoptilolite catalyst is comparable with the best results reported in literature.

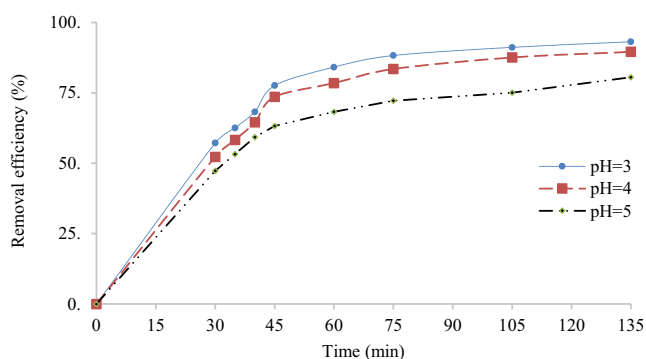


Fig. 5. Impacts of the initial pH on the photocatalytic degradation efficiency.

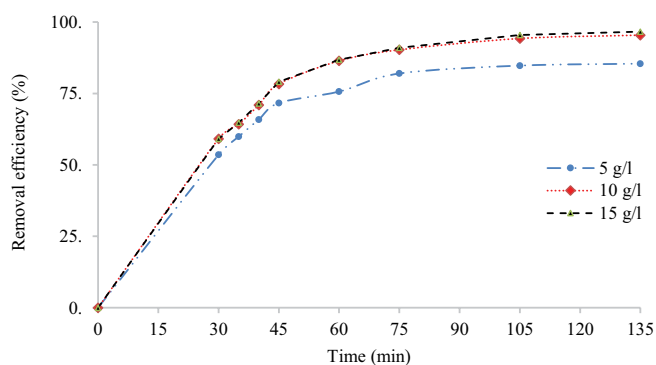


Fig. 6. Impacts of adsorbent dosage on the photocatalytic degradation efficiency.

3.4. Reusability of the photocatalyst

The photocatalytic degradation effectiveness of the modified sample after being reused for first time and second time is given in Fig. 8. Photocatalytic degradation stage of the used catalyst was determined after being washed with water and dried at 25°C. Efficiency of initial use was assessed 95.4% whereas second reuse resulted in a reduction of 83.4%. This decrease is due to adsorption of organic intermediates of photocatalytic degradation reaction in the photocatalyst's surface pores. Consequently, this influences the surface activity of the catalyst. Overall, outcomes illustrate that the photocatalyst is useful after being recycled, which is significant for real-world applications.

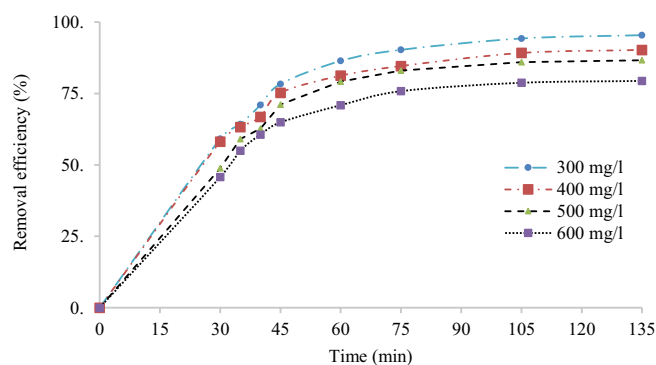


Fig. 7. Impacts of dye concentrations on the photocatalytic degradation efficiency.

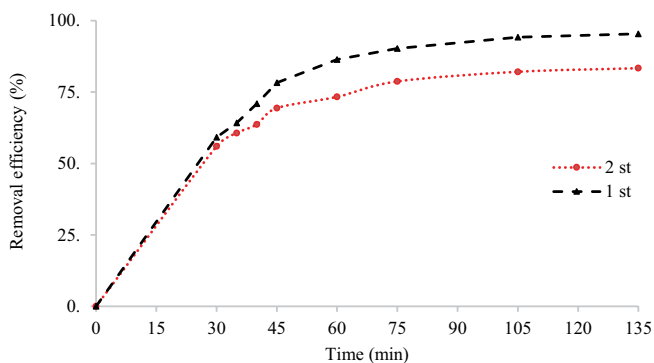


Fig. 8. Photocatalytic decolorization efficiency after the 1st and 2nd reuse of sample 30.

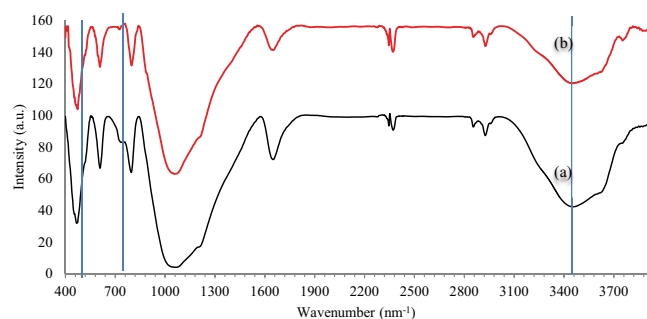


Fig. 9. Fourier-transform infrared spectra of sample 30 before (a) and after (b) photocatalytic decolorization.

3.5. Photocatalytic degradation activity

Fig. 9 presents the FTIR spectra of sample 30 before and after photo-activity. The hydroxyl groups cause the most noticeable variations in given spectrum at about 3400 cm^{-1} . After adsorption of Methylene Blue in absence of light, the strength of this peak was significantly lowered. This is due to adsorption of Methylene Blue by the catalyst agent. After being irradiated by light, no evidence demonstrating the presence of Methylene Blue functional group on catalyst was observed. The catalyst's effectiveness is thus revealed by degradation of the Methylene Blue on the catalyst's surface.

4. Conclusions

Clinoptilolite with exchanged zinc was obtained using solid-state ion-exchange process. SEM and XRD results revealed that when clinoptilolite is replaced with zinc, neither the crystal structure of the parent clinoptilolite nor the morphology are changed. As a result of the collapse of the pore structure during this process, N_2 adsorption tests on zinc-exchanged clinoptilolite an increase in surface area. The MB photocatalytic decolorization tests indicated a rapid degradation of the dye by zinc exchanged clinoptilolite, particularly sample 30. At $\text{pH} = 3$ and a catalyst concentration of 10 g/L of the modified zeolite, photocatalytic decolorization of Methylene Blue dye (300 ppm) achieved the best efficiency (95.4%). Reusability of the photocatalyst is demonstrated by the results, which is significant for practical applications. Therefore, zinc exchanged

clinoptilolite are capable of useful applications in the removal of this dye from wastewaters.

References

- [1] A. Nezamzadeh-Ejhieh, H. Zabihi-Mobarakeh, Heterogeneous photodecolorization of mixture of Methylene Blue and bromophenol blue using CuO -nano-clinoptilolite, *J. Ind. Eng. Chem.*, 20 (2014) 1421–1431.
- [2] Y. Costa-Marrero, M.B. de Andrade, J. Ellena, J. Duque-Rodríguez, T. Fariás, G. Autié-Castro, Zeolite/ ZnO composites based on a Cuban natural clinoptilolite and preliminary evaluation in Methylene Blue adsorption, *Mater. Res. Express*, 7 (2020) 015066, doi: 10.1088/2053-1591/ab6a5c.
- [3] A. Badeenezhad, A. Azhdarpoor, S. Bahrami, S. Yousefinejad, Removal of Methylene Blue dye from aqueous solutions by natural clinoptilolite and clinoptilolite modified by iron oxide nanoparticles, *Mol. Simul.*, 45 (2019) 564–571.
- [4] Y. Chen, K. Wang, L. Lou, Photodegradation of dye pollutants on silica gel supported TiO_2 particles under visible light irradiation, *J. Photochem. Photobiol., A*, 163 (2004) 281–287.
- [5] D. Ma, H. Yi, C. Lai, X. Liu, X. Huo, Z. An, L. Li, Y. Fu, B. Li, M. Zhang, L. Qin, Critical review of advanced oxidation processes in organic wastewater treatment, *Chemosphere*, 275 (2021) 130104, doi: 10.1016/j.chemosphere.2021.130104.
- [6] E.Y. Shaba, J.O. Jacob, J.O. Tijani, M.A.T. Suleiman, A critical review of synthesis parameters affecting the properties of zinc oxide nanoparticle and its application in wastewater treatment, *Appl. Water Sci.*, 11 (2021) 1–41.
- [7] P. Li, F. Liu, Y. Liu, R. Xue, X. Fan, Preparation and photocatalytic activity of visible light-responsive zinc oxide/activated carbon fiber composites, *J. Dispersion Sci. Technol.*, 42 (2021) 846–857.
- [8] A.S. Yasin, D. Hyun Kim, K. Lee, One-pot synthesis of activated carbon decorated with ZnO nanoparticles for capacitive deionization application, *J. Alloys Compd.*, 870 (2021) 159422, doi: 10.1016/j.jallcom.2021.159422.
- [9] A. Ruiz-Baltazar, R. Esparza, M. Gonzalez, G. Rosas, R. Pérez, Preparation and characterization of natural zeolite modified with iron nanoparticles, *J. Nanomater.*, 5 (2015) 1–8.
- [10] Z. Lei, J. Yang, X. Weiwei, S. Hao, L. Zhang, S. Qiang, Y. Yao, L. Xi, S. Shuangyan, Application and removal mechanism of ZnO /bentonite desulfurizer in the dry desulfurization, *Appl. Phys. A*, 128 (2022) 1–9.
- [11] B. Hakimi, M. Ghorbanpour, A. Feizi, A comparative study between photocatalytic activity of ZnO /bentonite composites prepared by precipitation, liquid-state ion-exchange and solid-state ion-exchange methods, *J. Water Environ. Nanotechnol.*, 3 (2018) 273–278.
- [12] S. Lotfiman, M. Ghorbanpour, Antimicrobial activity of ZnO /silica gel nanocomposites prepared by a simple and fast solid-state method, *Surf. Coat. Technol.*, 310 (2017) 129–133.
- [13] J.X. Ren, J.L. Zhu, S.C. Shi, M.Q. Yin, H.D. Huang, Z.M. Li, *In-situ* structuring a robust cellulose hydrogel with ZnO/SiO_2 heterojunctions for efficient photocatalytic degradation, *Carbohydr. Polym.*, 296 (2022) 119957, doi: 10.1016/j.carbpol.2022.119957.
- [14] M.C. Diaz-Nava, M.T. Olgúin, M. Solache-Ríos, M.T. Alarcón-Herrera, A. Aguilar-Elgueazabal, Characterization and improvement of ion-exchange capacities of Mexican clinoptilolite-rich tuffs, *J. Incl. Phenom. Macrocycl. Chem.*, 51 (2005) 231–240.
- [15] N. Mansouri, N. Rikhtegar, H.A. Panahi, F. Atabi, B.K. Shahraki, Porosity, characterization and structural properties of natural zeolite-clinoptilolite-as a sorbent, *Environ. Prot. Eng.*, 39 (2013) 139–152.
- [16] M. Akgül, Enhancement of the anionic dye adsorption capacity of clinoptilolite by Fe^{3+} -grafting, *J. Hazard. Mater.*, 267 (2014) 1–8.
- [17] K. Pourreza, S. Sharifnia, M. Khatamian, B. Rezaei, Effect of cation exchange on the performance of clinoptilolite mineral in the ethanol dewatering process, *Adsorpt. Sci. Technol.*, 29 (2011) 861–870.

- [18] A. Seidel, G. Kampf, A. Schmidt, B. Boddenberg, Zeolite ZnY catalysts prepared by solid-state ion-exchange, *Catal. Lett.*, 51 (1998) 213–218.
- [19] N. Garshasbi, M. Ghorbanpour, A. Nouri, S. Lotfiman, Preparation of zinc oxide-nanoclay hybrids by alkaline ion-exchange method, *Braz. J. Chem. Eng.*, 34 (2017) 1055–1063.
- [20] M. Ghorbanpour, Soybean oil bleaching by adsorption onto bentonite/iron oxide nanocomposites, *J. Phys. Sci.*, 29 (2018) 113–119.
- [21] B. Hakimi, M. Ghorbanpour, A. Feizi, ZnO/bentonite nanocomposites prepared with solid-state ion-exchange as photocatalysts, *J. Ultrafine Grained Nanostruct. Mater.*, 51 (2018) 139–146.
- [22] H. Pouraboulghasem, M. Ghorbanpour, R. Shayegh, S. Lotfiman, Synthesis, characterization and antimicrobial activity of alkaline ion-exchanged ZnO/bentonite nanocomposites, *J. Cent. South Univ.*, 23 (2016) 787–792.
- [23] N. Hajipour, M. Ghorbanpour, A. Feizi, Photo-Fenton decolorization of dye with Cu solid state exchanged bentonite, *Desal. Water Treat.*, 256 (2022) 265–272.
- [24] R. Shayegh, M. Ghorbanpour, A new approach for preparation of iron oxide-pillared bentonite as adsorbent of dye, *Desal. Water Treat.*, 183 (2020) 404–412.
- [25] N. Hajipour, M. Ghorbanpour, M. Safajou-Jahankhanemlou, Synthesis and characterization of solid-state Fe-exchanged nano-bentonite and evaluation of methyl orange adsorption, *Environ. Sci. Pollut. Res.*, 29 (2022) 49898–49907.
- [26] N. Hajipour, M. Ghorbanpour, A. Feizi, Application of photo-Fenton dye removal with gamma-Fe₂O₃/bentonite nanocomposites prepared by solid-state reaction in wastewater treatment, *Desal. Water Treat.*, 233 (2021) 311–318.